Available online at www.sciencedirect.com
SCIENCE DIRECT®
International Journal of Mass Spectrometry 241 (2005) 133–138
International Journal of Mass Spectrometry
www.elsevier.com/locate/ijms

The dissociation energy of $Cl_2O_2^+$

John M. Bailey, Changtong Hao, Brian J. Johnson, Lee S. Sunderlin*

Department of Chemistry and Biochemistry, Northern Illinois University, DeKalb, IL 60115, USA

Received 7 November 2004; accepted 13 December 2004
Available online 6 January 2005

Abstract

Crystal structures containing a trapezoidal $Cl_2O_2^+$ cation, one of several structural isomers of $Cl_2O_2^+$, have been recently obtained by the Seppelt group. There is no experimental thermochemistry for this isomer, partly because the corresponding neutral structure has no significant interdiatomic bonding. We have measured the 0 K dissociation energy $D(Cl_2^+–O_2) = 57 \pm 7$ kJ/mol using energy resolved collision-induced dissociation experiments in a flowing afterglow-tandem mass spectrometer. This leads to $\Delta_f H_{298}(Cl_2O_2^+) = 1056 \pm 7$ kJ/mol. The calculated B3LYP/aug-cc-pVTZ dissociation energy is 13 kJ/mol higher than experiment, while CASPT2 calculations by Seppelt and coworkers give a result 8 kJ/mol below experiment. The agreement between experiment and theory is better than for the related X_4^+ (X = Cl, Br, and I) cations.

Keywords: Flowing afterglow; Collision-induced dissociation; Bond dissociation energy; ab initio calculations

1. Introduction

Seppelt and coworkers recently reported the crystal structures of $Cl_2O_2^+SbF_6^-$, $Cl_2O_2^+Sb_2F_{11}^-$, and $Cl_2O_2^+$-$HIr_2F_{12}^-$ [1,2]. These three compounds contain $Cl_2O_2^+$ cations with similar trapezoidal structures. As shown in Fig. 1, the experimental structure resembles O_2 and Cl_2 moieties with a long interdiatomic distance. Computations indicate that the trapezoid is the lowest-energy structure for isolated $Cl_2O_2^+$ [2]. The next-lowest isomer, $ClOOCl^+$, is the ionized form of the ClOOCl intermediate important in the atmospheric depletion of ozone [3,4].

In a separate study, Cacace et al. [5] prepared two isomers of $Cl_2O_2^+$ in the gas phase by chemical ionization, and characterized them by means of collision-induced dissociation (CID) in a mass spectrometer. The first isomer of $Cl_2O_2^+$ was prepared by the chlorination of ClO_2, and the following reaction sequence was given as the most probable.

$$Cl_2^+ + Cl_2 \rightarrow Cl_3^+ + Cl \quad (1)$$

$$Cl_3^+ + ClO_2 \rightarrow Cl_2O_2^+ + Cl_2 \quad (2)$$

The dissociation of $Cl_2O_2^+$ yielded peaks for Cl^+, ClO^+, and ClO_2^+. This supports an open chain structure of $[ClOClO]^+$ because all fragments can be traced to the simple fission of one bond in the chain.

Cacace prepared the second isomer of $Cl_2O_2^+$ by association of Cl_2^+ with O_2. Eqs. (3) and (4) show the most likely reactions.

$$Cl_2^+ + O_2 \rightarrow Cl_2O_2^+ \quad (3)$$

$$Cl_2 + O_2^+ \rightarrow Cl_2O_2^+ \quad (4)$$

Reaction (3) is believed to be dominant because of a higher abundance of Cl_2^+ (recombination energy 11.480 eV) compared to O_2^+ (recombination energy 12.071 eV). Cacace et al. [5] presented evidence that the isomer of $Cl_2O_2^+$ that was prepared by association of Cl_2^+ with O_2 had the connectivity of the $Cl_2O_2^+$ cation isolated in the solid phase. This was supported by the dominance of Cl_2^+ and O_2^+ in the CID spectrum. Because there is no experimental thermochemistry for this isomer of $Cl_2O_2^+$, we performed energy-resolved CID measurements on this ion.

Trapezoidal $Cl_2O_2^+$ is related to the X_4^+ (X = halogen) radical cations. The Seppelt group has also determined a crystal structure for Cl_4^+, and our group has measured

* Corresponding author. Tel.: +1 815 753 6870; fax: +1 815 753 4802.
E-mail address: sunder@niu.edu (L.S. Sunderlin).

1387-3806/$ – see front matter © 2004 Elsevier B.V. All rights reserved.
doi:10.1016/j.ijms.2004.12.019

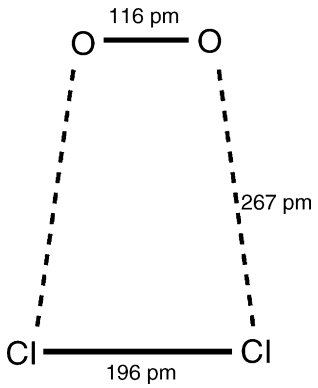

Fig. 1. Computed (B3LYP/aug-cc-pVTZ) geometry for $Cl_2O_2^+$.

dissociation enthalpies for X = Cl, Br, and I [6]. $Cl_2O_2^+$ is a weakly bound radical cation, like X_4^+. However, $Cl_2O_2^+$ has less symmetry (C_{2v} instead of D_{2h}), and one of the dissociation products (O_2) has a triplet ground electronic state. Computational difficulties with spin contamination have been noted for F_4^+, particularly in conformations with less symmetry [7]. Such problems are also likely for $Cl_2O_2^+$.

Li and Ng [8] performed G2 calculations of several isomers of Cl_2O_2 and $Cl_2O_2^+$. However, because their main concern was species of atmospheric interest, they did not report results for the neutral or cationic trapezoidal systems. Schwell and coworkers performed photoionization mass spectrometry studies of ClOOCl, determining $\Delta_f H(ClOOCl^+) = 1203 \pm 12$ kJ/mol [9].

2. Methods

2.1. Experimental

The strength of the Cl_2^+–O_2 interaction was measured using the energy-resolved collision-induced dissociation (CID) technique [10,11] in a flowing afterglow-tandem mass spectrometer (MS) [12]. The instrument consists of an ion source region, a flow tube, and the tandem MS. The dc discharge ion source used in these experiments is typically set at 2000 V with 2 mA of emission current. The flow tube is a 92 cm × 7.3 cm i.d. stainless steel pipe that operates at a buffer gas pressure of 0.35 Torr, a flow rate of 200 standard cm^3/s, and an ion residence time of 100 ms. The buffer gas is helium with up to 10% argon added to stabilize the dc discharge.

The $Cl_2O_2^+$ ions used in this study were prepared in the flow tube using the procedure of Cacace et al. [5] shown in Eqs. (3) and (4). Approximately 10^5 collisions with the buffer gas cool the resulting metastable $Cl_2O_2^+$ cluster ions to room temperature.

The tandem MS includes a quadrupole mass filter, an octopole ion guide, a second quadrupole mass filter, and a detector, contained in a stainless steel box that is partitioned into five differentially pumped interior chambers. During CID experiments, the ions are extracted from the flow tube and focused into the first quadrupole for mass selection. The reactant ions are then focused into the octopole, which passes through a reaction cell that contains a collision gas. After the dissociated and unreacted ions pass through the reaction cell, the second quadrupole is used for mass analysis. The detector is an electron multiplier operating in pulse-counting mode.

The energy threshold for CID is determined by modeling the cross section for product formation as a function of the reactant ion kinetic energy in the center-of-mass (CM) frame, E_{cm}. The octopole is used as a retarding field analyzer to measure the reactant ion beam energy zero. The ion kinetic energy distribution for the present data is typically Gaussian with a full-width at half-maximum of 0.9 ± 0.2 eV (1 eV = 96.5 kJ/mol). The octopole offset voltage measured with respect to the center of the Gaussian fit gives the laboratory kinetic energy, E_{lab}, in eV. Low offset energies are corrected for truncation of the ion beam [13]. To convert to the center-of-mass (CM) frame, the equation $E_{cm} = E_{lab} m(m+M)^{-1}$ is used, where m and M are the masses of the neutral and ionic reactants, respectively. All experiments were performed with both mass filters at low resolution to improve ion collection efficiency and reduce mass discrimination. Average atomic masses were used for all elements.

One complication with $Cl_2O_2^+$ is that another ion with a similar mass, Cl_3^+, is also created in the ion source. The main isotopic peaks of $Cl_2O_2^+$ are at 102, 104, and 106 amu, while the main peaks of Cl_3^+ are at 105, 107, 109, and 111 amu. In the present experiments, the first quadrupole was set to low resolution at a relatively low mass setting such that no ions heavier than 104 were transmitted. This avoided interference from Cl_3^+. The average reactant mass used was adjusted to account for the actual distribution of the transmitted ions.

Collision-induced dissociation data collected for weakly bound ions can give data that is difficult to fit because several of the assumptions made in the fitting procedure are less valid near zero energy in the laboratory frame [13]. These effects can cause measured thresholds to be too low. This problem can be alleviated by using a lighter collision gas. On the other hand, energy transfer during collisions with light collision partners like Ne can be less efficient, giving thresholds that are too high [14,15]. Therefore, CID experiments with $Cl_2O_2^+$ were done with both Ar and Ne as collision gases.

The total cross section for a reaction, σ_{total}, is calculated using $I = I_0 \exp(-\sigma_{total} nl)$, where I is the intensity of the reactant ion beam, I_0 is the intensity of the incoming beam ($I_0 = I + \sum I_i$), I_i is the intensity of each product ion, n is the number density of the collision gas, and l is the effective collision length, 13 ± 2 cm. Individual product cross sections σ_i are equal to $\sigma_{total}(I_i/\sum I_i)$. Data taken at several pressures is extrapolated to a zero pressure cross section before fitting the data to avoid the effects of secondary collisions [16].

Threshold energies are derived by fitting the data to a model function given in Eq. (5), where $\sigma(E)$ is the cross section for formation of the product ion at center-of-mass energy E, E_T is the desired threshold energy, σ_0 is the scaling factor,

Table 1
Vibrational frequencies, rotational constants, and polarizabilities

	Calculated[a]	Experimental[b]
$Cl_2O_2^+$ vib	109, 140, 160, 330, 582, 1684	
$Cl_2O_2^+$ rot	0.0732, 0.1106, 0.2162	
Cl_2^+ vib	626	646
Cl_2^+ rot	0.261	0.270
O_2 vib	1626	1580
O_2 rot	1.450	1.438
O_2 pol	7.45	

All values in cm^{-1} except polarizability in $Å^3$.
[a] B3LYP/aug-cc-pVTZ results.
[b] Reference [23].

n is an adjustable parameter, and i denotes rovibrational states having energy E_i and population $g_i(\sum g_i = 1)$. Doppler broadening and the kinetic energy distribution of the reactant ion are also accounted for in the data analysis, which is done using the CRUNCH program written by Armentrout and coworkers [13].

$$\sigma(E) = \frac{\sigma_0 \sum_i g_i(E + E_i - E_T)^n}{E} \quad (5)$$

Experimental vibrational frequencies are not available for $Cl_2O_2^+$. Therefore, vibrational and rotational frequencies for reactants and products were calculated using the B3LYP model [17] and the aug-cc-pVTZ basis set [18] to give a consistent set of frequencies, given in Table 1. This method gives generally good frequencies for this purpose [6,19,20]; the calculated values for Cl_2^+ and O_2 agree with experimental values (Table 1) within 3%. Uncertainties in the derived thresholds due to possible inaccuracies in the frequencies were estimated by multiplying the entire sets of frequencies by 0.9 and 1.1. The resulting changes in internal energies are less than 1 kJ/mol. Therefore, the calculated frequencies were used without scaling. The polarizability of the neutral product was also taken from the computational results; varying this parameter has a negligible effect on the derived energetics.

Collisionally activated metastable complexes can have sufficiently long lifetimes that they do not dissociate on the experimental timescale (ca. 50 μs). Such kinetic shifts are accounted for in the CRUNCH program by RRKM lifetime calculations, where the reaction transition states are presumed to be essentially product-like [21]. The uncertainty in the derived thresholds is again estimated by multiplying reactant or product frequency sets by 0.9 and 1.1, and by multiplying the time window for dissociation by 10 and 0.1. The kinetic shift for this molecule is small and the effect of these variations is less than 1 kJ/mol.

Cl_2 was obtained from Specialty Gas Group. He, Ar, and O_2 were obtained from BOC, and Ne was obtained from Matheson Gas Products. All reagents were used as received.

2.2. Computational

All computational work on these systems was performed using the Gaussian 98 Suite [22]. All calculations involving radicals were performed with unrestricted wavefunctions. Geometry optimizations were performed with tight convergence criteria, and all species discussed were found to have no imaginary frequencies (they are stable minima). Most calculations on $Cl_2O_2^+$ using a variety of methods including MP2 and CBS-Q were unsuccessful because of spin contamination in the calculated wavefunctions [7]. However, calculations using the B3LYP/aug-cc-pVTZ method were successful; the results are reported in Section 3, along with previously reported results.

3. Results and discussion

3.1. Experimental results

CID of $Cl_2O_2^+$ gives reaction (6) as the only observed product.

$$Cl_2O_2^+ \rightarrow Cl_2^+ + O_2 \quad (6)$$

The appearance curve and fits to the data are shown in Fig. 2. The Eq. (5) fitting parameters for argon collision gas ($n = 1.1 \pm 0.1$, $E_T = 0.57 \pm 0.06$ eV) and neon collision gas ($n = 1.3 \pm 0.1$, $E_T = 0.60 \pm 0.05$ eV) are similar. The effects of reactant and product internal energy are included in the fitting procedure, so the dissociation thresholds correspond to an energy at 0 K. The final uncertainty in the energy is derived from the standard deviation of the thresholds determined for individual data sets, the uncertainty in the reactant internal energy, the effects of kinetic shifts, and the uncertainty in the energy scale (±0.15 eV lab). These results are given in Table 2, along with results calculated at various levels of theory.

We attempted to make $F_2O_2^+$, $Br_2O_2^+$, and $I_2O_2^+$ by the same technique with different dihalogen precursors, but it was not possible to make these ions, at least in quantities greater than background impurities. Cl_2 and O_2 have similar ionization energies, while the other halogens are substantially

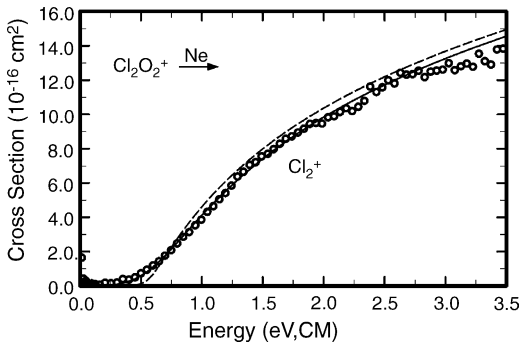

Fig. 2. Cross section for collision-induced dissociation of $Cl_2O_2^+$ as a function of energy in the center-of-mass frame. The solid and dashed lines represent convoluted and unconvoluted fits ($E_T = 0.61$ and $n = 1.31$) to the data, as discussed in the text.

Table 2
Experimental and computed dissociation energies for $Cl_2O_2^+$

Method	BDE (kJ/mol)
Experimental[a]	58 ± 6
Experimental[b]	55 ± 7
Experimental[c]	57 ± 7
CASPT2[d]	49.1
B3LYP/6–311++G(3df,3pd)[e]	77.4
B3LYP/aug-cc-pVTZ[f]	69.9

[a] Neon collision gas.
[b] Argon collision gas.
[c] Final average experimental value.
[d] Reference [2] value with zero point energy correction from B3LYP/aug-cc-pVTZ frequencies.
[e] Reference [2].
[f] This work.

different [23]. Homodimeric radical cations are generally more stable than heterodimeric systems [7]; apparently, more equal sharing of charge between Cl_2 and O_2 leads to stronger bonding.

3.2. Computationally predicted geometries

Experimental and calculated bond lengths in $Cl_2O_2^+$ are given in Table 3. The three crystal structures give similar geometries, suggesting that the structure is reasonably robust and not greatly affected by the counterion. The CASPT2 results are in good agreement with experiment, as previously noted [2]. The B3LYP results are also in reasonable agreement except for the O–Cl distance, where the computed value is substantially larger than the experimental value. This is the same trend seen in the Cl_4^+ results [6].

The experimental Cl–Cl bond length is essentially equal to the shorter experimental value for Cl_2^+ rather than the longer value for Cl_2 [2]. Conversely, the experimental and calculated O–O bond lengths are closer to the value for O_2, except for the B3LYP results. Thus, the experimental and CASPT2 bond lengths suggest that the Cl_2 moiety in $Cl_2O_2^+$ has most of the charge, while the B3LYP results suggest a more equal sharing of the charge.

Table 3
Bond lengths (pm) in $Cl_2O_2^+$

Method	O—O	Cl—Cl	O—Cl
$Cl_2O_2^+SbF_6^-$ xrd[a]	118.5	191.6	242.5
$Cl_2O_2^+Sb_2F_{11}^-$ xrd[a]	120.7	190.9	242.4
$Cl_2O_2^+HIr_2F_{12}^-$ xrd[b]	116	189	244
CASPT2[a]	122	190.6	242
B3LYP/6–311+G(3df)[a]	116.1	194.5	264.7
B3LYP/aug-cc-pVTZ[c]	116.2	196.0	266.5
Diatomic neutral exp[d]	120.8	198.7	–
Diatomic cation exp[d]	111.6	189.1	–

xrd = X-ray diffraction data.
[a] Reference [2].
[b] Reference [1].
[c] This work.
[d] Reference [23].

3.3. Atomic charges and spin densities

Seppelt and coworkers [2] derived charges of +0.21 on O and +0.29 on Cl by using the CASPT2 method. They obtained similar values of +0.17 on O and +0.33 on Cl with the B3LYP/cc-pVTZ//CASPT2 model. We calculated values of +0.19 and +0.31, respectively, with the B3LYP/aug-cc-pVTZ model, in good agreement with the other calculated charges.

The calculated charges agree with the suggestion from the geometry calculations that the chlorine atoms have the majority of the charge. However, the direct B3LYP calculations show greater chlorine charges than the CASPT2 calculations, in contrast to the trend implied by the calculated geometries. Considering the model dependence of the calculated charges and the geometry-charge correlations, the discrepancies are not surprising.

The EPR spectrum of $Cl_2O_2^+$ suggests that "the unpaired electron resides largely on the chlorine atoms" [2]. According to the CASPT2 results, the SOMO is mostly a dioxygen π^* orbital, while the B3LYP/cc-pVTZ//CASPT2 model indicates 62% of the spin density is on the Cl_2 moiety [2]. Our B3LYP/aug-cc-pVTZ calculations indicate 0.75 unpaired electrons on each oxygen atom and 0.25 unpaired electrons on each chlorine atom with the opposite spin. This is consistent with $Cl_2O_2^+$ being a nearly equal mixture of two resonance structures $[^3O_2{-}^2Cl_2^+] \leftrightarrow [^2O_2^+{-}^1Cl_2]$, with low-spin coupling in the first resonance structure to give an overall doublet state. However, the differences between these results suggests that the electronic structure of $Cl_2O_2^+$ is not yet fully characterized.

3.4. Dissociation energies

CID experiments with Ne and Ar give respective dissociation energies of 58 ± 6 and 55 ± 7 kJ/mol for $Cl_2O_2^+$. The fact that Ar gives a lower value than Ne is consistent with the likely systematic errors discussed in Section 2.1. However, the two values are well within the experimental uncertainty of each other, suggesting that any systematic error due to the nature of the collision gas is minimal. The best experimental dissociation threshold is therefore taken to be the average of all the data, 57 ± 7 kJ/mol. The uncertainty here includes the effects of other sources of error as discussed in Section 2.1.

The experimental 0 K dissociation energy can be used to derive a 298 K dissociation enthalpy using the integrated heat capacities of the reactants and products, which are determined using the frequencies in Table 1. These give a 298 K dissociation enthalpy that is slightly larger, 58 ± 7 kJ/mol.

This dissociation energy was previously calculated using two methods. CASPT2 calculations gave 54 kJ/mol without zero point energy correction, which can be converted to a 0 K dissociation energy of 49 kJ/mol using the B3LYP/aug-cc-pVTZ frequencies. This is in reasonable agreement with the experimental results. The B3LYP/6–311++G(3df,3pd) method gave a dissociation energy of 77 kJ/mol, 20 kJ/mol higher than the experimental value. Energy calculations

performed with the B3LYP method and a different large basis set, aug-cc-pVTZ, give a dissociation energy that is somewhat lower, 70 kJ/mol. In comparison, B3LYP calculations with large basis sets overestimate the experimental dissociation energy in Cl_4^+ by 40 kJ/mol. Thus, the B3LYP value for the $Cl_2O_2^+$ dissociation energy is in significantly better agreement with experiment than the corresponding Cl_4^+ value. This is consistent with the less symmetric $Cl_2O_2^+$ system being more amenable to computational methods.

The Cl_2^+–O_2 dissociation energy can be used to determine the heat of formation of $Cl_2O_2^+$. The gas-phase heats of formation of Cl_2, O_2, and the electron are zero at 298 K. The ionization energy of Cl_2 is 11.481 eV, or 1108 kJ/mol [24]. This gives an ionization enthalpy at 298 K of 1114 kJ/mol, where heat capacities were determined using the experimental vibrational frequencies of 646 cm^{-1} for Cl_2^+ and 560 cm^{-1} for Cl_2 [23]. (This value uses the 'ion convention', where the electron is treated as having the heat capacity of an ideal gas [25].) The heat of formation of Cl_2^+ is therefore 1114 kJ/mol at 298 K. The dissociation enthalpy of 58 ± 7 kJ/mol can be subtracted from this value to give $\Delta_f H_{298}(Cl_2O_2^+) = 1056 \pm 7$ kJ/mol. This is 147 kJ/mol lower in energy than $\Delta_f H_{298}(ClOOCl^+) = 1203 \pm 12$ kJ/mol [9]. For comparison, the lowest-energy structure for neutral Cl_2O_2 is calculated at the modified G2 level to be a loosely bound complex of Cl_2 and O_2 [26], but it has a "hockey stick" structure rather than a trapezoidal structure like the ion. Neutral ClOOCl is calculated to be 136 kJ/mol higher in energy [26], a difference similar to that seen in the ionic systems.

3.5. Spin-orbit coupling

There are two spin-orbit states of Cl_2^+, $^2\prod_{3/2}$ and $^2\prod_{1/2}$. The $^2\prod_{3/2}$ state is lower in energy by 0.095 eV [24]. The $^2\prod_{3/2}$ and $^2\prod_{1/2}$ states of O_2^+ differ in energy by less, 0.024 eV [23]. The low-lying term energies of the ^2A ground state [2] of $Cl_2O_2^+$ are not known experimentally, but the energy difference is presumably no larger than these two values. The calculated dissociation energies (except for the CASPT2 results) refer to a weighted average of the spin-orbit states (67% $J = 3/2$ and 33% $J = 1/2$ for the diatomics). The experimental dissociation energy is modeled assuming ground electronic states for the reactant and products, but it is possible that some of the reactants or products are in higher energy levels. Thus, the experimental and computational results refer to states (or distributions of states) that may be different by up to roughly 0.03 eV. This is a small contribution to the overall uncertainties.

4. Conclusions

The 0 K dissociation energy $D(Cl_2$–$O_2^+)$ has been measured to be 57 ± 7 kJ/mol using energy-resolved collision-induced dissociation. CASPT2 and B3LYP/aug-cc-pVTZ results are in reasonable agreement with experiment. The trapezoidal isomer is lower in energy than the chain $ClOOCl^+$ isomer by about 150 kJ/mol.

Acknowledgments

We thank Peter Armentrout, Mary Rodgers, and Kent Ervin for use of the CRUNCH software for data analysis, and a reviewer for helpful comments.

References

[1] S. Seidel, K. Seppelt, Angew. Chem. Int. Ed. 39 (2000) 3923.
[2] T. Drews, W. Koch, K. Seppelt, J. Am. Chem. Soc. 121 (1999) 4379.
[3] L.T. Molina, M.J. Molina, J. Phys. Chem. 91 (1987) 433.
[4] J. Plenge, R. Flesch, S. Kühl, B. Vogel, R. Müller, F. Stroh, E. Rühl, J. Phys. Chem. A 108 (2004) 4859.
[5] F. Cacace, G. Petris, A. Troiani, Rapid Commun. Mass Spectrom. 13 (1999) 1903.
[6] J.M. Bailey, C. Hao, K.S. Frusolone, C.E. Check, T.M. Gilbert, L.S. Sunderlin, J. Phys. Chem. A, submitted for publication.
[7] P.C. Hiberty, N. Berthe-Gaujac, J. Phys. Chem. A 102 (1998) 3169.
[8] W.-K. Li, C.-Y. Ng, J. Phys. Chem. A 101 (1997) 113.
[9] M. Schwell, H.-W. Jochims, B. Wassermann, U. Rockland, R. Flesch, E. Rühl, J. Phys. Chem. 100 (1996) 10070.
[10] F. Muntean, P.B. Armentrout, J. Chem. Phys. 115 (2001) 1213.
[11] P.B. Armentrout, J. Am. Soc. Mass Spectrom. 13 (2002) 419.
[12] K. Do, T.P. Klein, C.A. Pommerening, L.S. Sunderlin, J. Am. Soc. Mass Spectrom. 8 (1997) 688.
[13] (a) K.M. Ervin, P.B. Armentrout, J. Chem. Phys. 83 (1985) 166; (b) M.T. Rodgers, K.M. Ervin, P.B. Armentrout, J. Chem. Phys. 106 (1997) 4499.
[14] N. Aristov, P.B. Armentrout, J. Phys. Chem. 90 (1986) 5135.
[15] P.B. Armentrout, Int. J. Mass Spectrom. 200 (2000) 219.
[16] (a) S.K. Loh, D.A. Hales, L. Lian, P.B. Armentrout, J. Chem. Phys. 90 (1989) 5466; (b) R.H. Schultz, K.C. Crellin, P.B. Armentrout, J. Am. Chem. Soc. 113 (1991) 8590.
[17] A.D. Becke, J. Chem. Phys. 98 (1993) 5648.
[18] (a) T.H. Dunning Jr., J. Chem. Phys. 90 (1989) 1007; (b) R.A. Kendall, T.H. Dunning Jr., R.J. Harrison, J. Chem. Phys. 96 (1992) 6796; (c) D.E. Woon, T.H. Dunning Jr., J. Chem. Phys. 98 (1993) 1358; (d) A.K. Wilson, D.E. Woon, K.A. Peterson, T.H. Dunning Jr., J. Chem. Phys. 110 (1999) 7667.
[19] C.E. Check, T.O. Faust, J.E. Bailey, B.J. Wright, T.M. Gilbert, L.S. Sunderlin, J. Phys. Chem. A 105 (2001) 8111.
[20] E.G. Robertson, D. McNaughton, J. Phys. Chem. A 107 (2003) 642.
[21] P.B. Armentrout, J. Simons, J. Am. Chem. Soc. 114 (1992) 8627.
[22] M.J. Frisch, G.W. Trucks, H.B. Schlegel, G.E. Scuseria, M.A. Robb, J.R. Cheeseman, V.G. Zakrzewski, J.A. Montgomery Jr., R.E. Stratmann, J.C. Burant, S. Dapprich, J.M. Millam, A.D. Daniels, K.N. Kudin, M.C. Strain, O. Farkas, J. Tomasi, V. Barone, M. Cossi, R. Cammi, B. Mennucci, C. Pomelli, C. Adamo, S. Clifford, J. Ochterski, G.A. Petersson, P.Y. Ayala, Q. Cui, K. Morokuma, A.D. Malick, K.D. Rabuck, K. Raghavachari, J.B. Foresman, J. Cioslowski, J.V. Ortiz, A.G. Baboul, B.B. Stefanov, G. Liu, A. Liashenko, P. Piskorz, I. Komaromi, R. Gomperts, R.L. Martin, D.J. Fox, T. Keith, M.A. Al-Laham, C.Y. Peng, A. Nanayakkara, M. Challacombe, P.M.W. Gill, B. Johnson, W. Chen, M.W. Wong, J.L. Andres, C. Gonzalez,

M. Head-Gordon, E.S. Replogle, J.A. Pople, Gaussian 98, Revision A.9, Gaussian Inc., Pittsburgh, PA, 1998.
[23] K.P. Huber, G. Herzberg, Constants of diatomic molecules (data prepared by J.W. Gallagher, R.D. Johnson III), in: P.J. Linstrom, W.G. Mallard (Eds.), NIST Chemistry WebBook, NIST Standard Reference Database Number 69, National Institute of Standards and Technology, Gaithersburg, MD, March 2003, p. 20899, http://webbook.nist.gov/.
[24] A.J. Yencha, A. Hopkirk, A. Hiraya, R.J. Donovan, J.G. Goode, R.R.J. Maier, G.C. King, A. Kvaran, J. Phys. Chem. 99 (1995) 7231.
[25] J.E. Bartmess, Negative ion energetics data, in: P.J. Linstrom, W.G. Mallard (Eds.), NIST Chemistry WebBook, NIST Standard Reference Database Number 69, National Institute of Standards and Technology, Gaithersburg, MD, March 2003, p. 20899, http://webbook.nist.gov/.
[26] R.S. Zhu, M.C. Lin, J. Chem. Phys. 118 (2003) 4094.